

Exocomets in the Proxima Centauri system and their importance for water transport

R. Schwarz,^{1*} Á. Bazsó,¹ N. Georgakarakos,² B. Loibnegger,¹ D. Bancelin,¹
E. Pilat-Lohinger,¹ K. G. Kislyakova,^{1,3} R. Dvorak,¹ T. I. Maindl,¹
and I. Dobbs-Dixon²

¹*Department of Astrophysics, University of Vienna, A-1180 Vienna, Türkenschanzstrasse 17, Austria*

²*New York University Abu Dhabi, PO Box 129188, Abu Dhabi, UAE*

³*Space Research Institute, Austrian Academy of Sciences, Schmiedlstrasse 6, A-8042 Graz, Austria*

Accepted XXX. Received YYY; in original form ZZZ

ABSTRACT

The scenario and the efficiency of water transport by icy asteroids and comets are still amongst the most important unresolved questions about the early phases of planetary systems. The detection of Proxima Centauri b (PCb), which moves in the habitable zone, triggered a debate whether or not this planet can be habitable depending on its formation history and available water content. A better understanding of cometary dynamics in extrasolar systems shall provide information about cometary reservoirs and give an insight into water transport especially to planets in the habitable zone.

In our study we perform numerous N-body simulations with PCb and an outer reservoir of comets. We investigate close encounters and collisions with the planet, which are important for the transport of water. Observers found hints for a second planet with a period up to 500 days. Our studies show that from the dynamical point of view two planets are stable even for a massive second planet with up to ~ 12 Earth masses. The simulations of a possible second planet yield that this planet can stay in a stable orbit very close to PCb. For the study of exocomets we include an additional planet outside of PCb in our calculations and we also consider the influence of the binary α Centauri.

The studies on the dynamics of exocomets reveal that the outer limit for water transport is between 100 and 200 au. From our simulations we estimate the water mass delivered to the planets to be between 0 and 30 Earth oceans.

Key words: stars: individual: Proxima Centauri – celestial mechanics – comets: general – (stars:) planetary systems – methods: numerical

1 INTRODUCTION

Comets in the Solar System are known to be a natural by-product of planet formation (Wahlberg Jansson & Johansen 2014; Willacy et al. 2015). It is assumed that comets formed beyond the snow-line (Mulders et al. 2015), and they have a higher water content than other minor bodies. Observations of comets (e.g., Hartogh et al. 2011; Altwegg et al. 2015) confirm that the deuterium-to-hydrogen (D/H) ratio of Solar System comets agrees with or exceeds the D/H ratio found in Earth’s oceans. These results of comet spectroscopy give a hint on water transport in the Solar System and could be relevant for studies beyond.

In a recent work of de la Fuente Marcos & de la Fuente Marcos (2017) they detected maybe an “exocomet” (A/2017 U1). They identified the interstellar minor body by its positive barycentric energy. The investigation of the kinematics of this exocomet by Mamajek (2017) showed that it does not appear to be associated with any local exo-Oort clouds (the triple system α and Proxima Centauri). One can conjecture that every planetary system should host cometary activity.

Observations by Beust et al. (1990) could support this assumption and showed indications of exo-cometary activity even before the first exoplanet was confirmed. They found a large number of metallic absorption lines in the spectra of β Pictoris which varied on short time scales. This was interpreted as clouds of gas and dust obscuring the light of the star produced by so called ‘falling evaporating bodies’.

* E-mail: richard.schwarz@univie.ac.at

Between 2003 and 2011 spectra of β Pictoris were gathered and then analysed by [Kiefer et al. \(2014b\)](#) who discovered about 6000 variable absorption features (Ca II H,K) possibly arising from clouds transiting the disk of the star. The idea of exocomets producing these clouds seems to be the most reasonable for explaining the observations so far. The same absorption features have been found in observations of many other star systems, such as HD 21620, HD 42111, HD 110411, and HD 145964, by [Welsh & Montgomery \(2013\)](#) who examined absorption profiles from 21 mainly young (~ 5 Myr) A-type stars with circumstellar disks. One can assume that these systems are still in the phase of planet formation and the changing gravitational field throws potentially large numbers of icy bodies from the outskirts inwards towards the central star. The radial velocities measured for the absorption features were in the range of ± 100 km s $^{-1}$. From the existence of comets one can assume that there exist also cometary reservoirs in other planetary systems in analogy to the Kuiper-belt or the Oort Cloud.

[Nilsson et al. \(2010\)](#) described the observation of 22 exo-Kuiper-belt candidates at a wavelength of 870 μ m with the LABOCA bolometer. Five of the debris disks observed with 3- σ significance have been detected for the first time. They argue that since dust has a limited lifetime, observations which prove its existence lead to the assumption that there are larger asteroidal and/or cometary bodies that continuously renew the amount of dust and form dusty debris disks through collisions. The role of comets in the delivery of water and basic organic material to planets – especially terrestrial planets – is still not well understood. This question is closely related to the possible habitability of planets in extrasolar systems.

Assuming that in other planetary systems comets play the same role as in our Solar System, we investigated the possibility of water transport by comets in the well discussed system of Proxima Centauri (e.g., [Anglada-Escudé et al. 2016](#); [Coleman et al. 2017](#); [Mesa et al. 2017](#)). At a distance of 1.295 parsecs, the red dwarf Proxima Centauri (M5.5V) is the Sun’s closest stellar neighbour and one of the best-studied low-mass stars. It is part of the triple star system including Alpha Centauri as shown in the work of [Kervella et al. \(2017\)](#). Proxima Centauri is an M-star with mass $M = 0.12 \pm 0.015 M_{\odot}$ separated by 8700 au from the binary system Alpha Centauri A & B. [Anglada-Escudé et al. \(2016\)](#) have announced the discovery of Proxima Centauri b (PCb), a terrestrial planet with a minimum mass of $1.3 M_{\oplus}$ orbiting the host star.

The data of PCb is collected in the catalogue of exoplanets in binary (multiple) star systems ([Schwarz et al. 2016](#))¹ which is available since 2013.

The properties of the planet are given in table 1. PCb is also interesting, because the planet orbits within the habitable zone (HZ) as shown in table 1 by using the work of [Kopparapu et al. \(2014\)](#).

There is a great debate whether or not the planet is habitable; e.g., [Ribas et al. \(2016\)](#) offer a broad overview on that topic. PCb is very close to the star which would induce a greenhouse effect and water vapour escape. Consideration of

Table 1. Orbital parameters of PCb and the location of the HZ in the Proxima Centauri system. The limits of the HZ are taken from the work of [Kopparapu et al. \(2014\)](#). Updates and statistics are presented in the catalogue of exoplanets in binaries and multiple star systems ([Schwarz et al. 2016](#)).

Name	a (au)	p (days)	e	m (M_{\oplus})
PCb	0.0485	11.186	0-0.3	1.27
Habitable zone*	0.045–0.119			

tidal heating requires an important refinement in the definition of the HZ, as in a general study of [Barnes et al. \(2009\)](#). Additionally for close in planets like in Trappist-1 the induction heating can melt the upper mantle and enormously increase volcanic activity, sometimes producing a magma ocean below the planetary surface ([Kislyakova et al. 2017](#)). This heating cloud lead to the complete loss of water from the planet, which may also happen for Proxima Centauri b.

The main goal of this work is to show whether water transport by comets is possible and to assess the contribution of cometary reservoirs with the help of dynamical investigations. In our investigations we assume that Proxima Centauri does have comet reservoirs with a fairly large water content.

The investigation of debris disks provides a useful insight into the origin of (exo)cometary reservoirs. Hence, the observation of exocomets is crucial which is shown in the work of e.g., [Grady et al. \(1997\)](#) (HD 100546), [Kiefer et al. \(2014a\)](#) (β Pictoris and HD 172555), and [Eiroa et al. \(2016\)](#) (ϕ Leonis). A former investigation by [Loibnegger & Dvorak \(2017\)](#) compared the dynamics of comets in two different systems, namely HD 10180 and HIP 14810. They found that the orbit of the most massive planet in the system has a large influence on the capture probability of comets.

The (exo)cometary reservoirs depend on the formation and evolution of the protoplanetary disk. [Ribas et al. \(2015\)](#) (page 8, Fig. 5) could show quantitatively that protoplanetary disks dissipate significantly faster and/or earlier around high mass stars, as they found between 10 and 30% more protoplanetary disks around low-mass stars regardless of the age. [Vicente & Alves \(2005\)](#) presented results on the size distribution of circumstellar disks in the Trapezium cluster measured from HST/WFPC2 data. In their Fig. 8 on page 12 the disk size is also presented for M stars like Proxima Centauri which would be around 100 au for the spectral type of M5.5V. The work of [Pawellek et al. \(2014\)](#) (page 11, Fig. 2) could confirm the result by studying a representative sample of 34 debris disks resolved in various Herschel Space Observatory programs to constrain the disk radii and the size distribution of their dust. These results are important for our initial conditions which we describe in section 2.2.

Besides the primary question of water transport by comets and the related dynamical habitability of PCb, another important dynamical question is: “Could there be a second planet in the Proxima Centauri system?” [Anglada-Escudé et al. \(2016\)](#) announced that there is maybe a second planet with orbital period of up to 500 days, but its nature is still unclear due to stellar activity and inadequate sampling. We have addressed this important issue in section 3.1, where

¹ <http://www.univie.ac.at/adg/schwarz/multiple.html>

we analysed the stability of a second planet. The paper is organized as follows: first we describe the model and methods of our studies (section 2), then we present the results of the stability of an additional planet (section 3.1), next we show the results of the study on the dynamics of exocomets (section 3.2), and estimate the limit of the possible water mass transport (section 3.3), as well as the summary (section 4).

2 MODELS AND METHODS

2.1 Stability of an additional planet

First we studied the possibility of an additional planet (planet c) being stable. To do this, we used the full 3-body problem (3BP) where we define the star (m_1) the planet PCb (m_2) and a possible second planet (m_3). We have regarded all the celestial bodies involved as point masses and integrated the equations of motion for the stability maps up to $T_c = 10^6$ periods of PCb. For our simulations we used the Lie integrator with adaptive step size control (see [Hanslmeier & Dvorak 1984](#); [Lichtenegger 1984](#); [Eggl & Dvorak 2010](#)). We computed the maximum eccentricity e_{\max} during the evolution of an orbit to determine its stability and also the region of stable motion around PCb (planet b). If any planet's (planet b or planet c) orbit becomes hyperbolic ($e_{\max} > 1$) the system is considered to be unstable. The global results of chaos indicators (e.g., LCI, FLI, RLI, ...) are in good agreement with the e_{\max} criterion as shown in [Schwarz et al. \(2009\)](#).

The initial conditions for PCb were set like in the paper of [Anglada-Escudé et al. \(2016\)](#) including the uncertainties: $a_2 = 0.0485$ au, $e_2 = 0, 0.1, 0.2$ and 0.3 , and an inclination of $i_2 = 0$ degree. The second planet (planet c) was started from $a_3 = 0.06$ au up to $a_3 = 0.3$ au (for test calculations up to 0.7 au); in addition we varied the initial eccentricity from $e_3 = 0$ up to $e_3 = 0.5$.

The estimates of the exoplanet's mass were conducted in the work of [Kane et al. \(2017\)](#) for three different (line-of-sight) inclination scenarios: 90° (edge on), 30° , and 10° (nearly face on). These inclinations imply a (minimum) mass for the known planet of $1.27, 2.54$, and $7.31 M_\oplus$, respectively. We set the masses of the planets (planet b and c) equal ($m_2 = m_3$) to decrease the number of free parameters and investigated the following masses:

- One mass of PCb ($1 M_{\text{Prox}}$) $m_2 = m_3 = 1.27 M_\oplus$,
- $5 M_{\text{Prox}}$ corresponding to $m_2 = m_3 = 6.35 M_\oplus$, and
- in addition we made tests for $10 M_{\text{Prox}}$ corresponding to $m_2 = m_3 = 12.7 M_\oplus$.

The last two masses correspond to super-Earth planets which are quite common. [Süli et al. \(2005\)](#) studied the stability of terrestrial planets with a more massive “Earth”. They found that stability of the Solar system depends on the masses of the planets, and small changes in these parameters may result in a different dynamical evolution of the planetary system.

Radial velocity

[Anglada-Escudé et al. \(2016\)](#) wrote, “that the presence of another super-Earth mass planet cannot yet be ruled out at longer orbital periods and Doppler semi-amplitudes

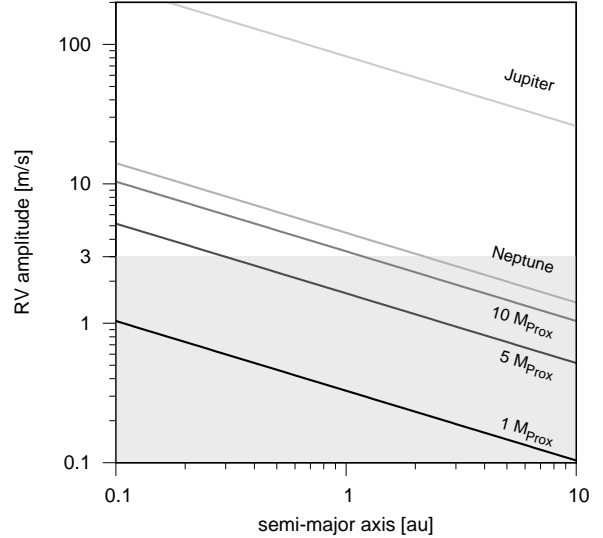


Figure 1. Estimate of the minimum (radial) velocity for Proxima Centauri for the detection of a possible second planet, depending on the mass and the distance of this planet. The lower three masses were used for the stability studies. The grey shaded region represents the observation limit which is $RV \approx 3 \text{ m s}^{-1}$ ([Anglada-Escudé et al. 2016](#)).

$\lesssim 3 \text{ m s}^{-1}$, whereas the Doppler semi-amplitude of Proxima b is $\approx 1.4 \text{ m s}^{-1}$.” Therefore we made an estimate by the help of Kepler’s third law to see which planets would be detectable also in the range of our calculations.

$$V_{\text{Prox}} \approx \left(\frac{m_3}{m_1} \sqrt{\frac{Gm_1}{a_3}} \right). \quad (1)$$

Equation 1 estimates the radial velocity for Proxima Centauri (V_{Prox} in m s^{-1}) for a possible second planet, which depends on the mass of the second planet c (m_3), the mass of the central star, the gravitational constant and the distance a_3 in (au) of planet c. Because of the radial velocity (RV) observations we do not expect a second planet with a mass larger than a super-Earth. Fig. 1 shows the RV amplitude limit in m s^{-1} for the different planet masses by using the limits of [Anglada-Escudé et al. \(2016\)](#). One can see that Neptune-sized planets could only be detected at distances ≤ 2 au.

The question of giant planets in exoplanetary systems is closely linked with the formation of Jupiter. [Kruijer et al. \(2017b\)](#) and [Kruijer et al. \(2017a\)](#) investigated this topic by doing W and Mo isotope analyses of iron meteorites. They studied 16 selected samples covering five different rare iron meteorite groups by using mass spectroscopy, and could show that Jupiter’s solid core must have formed within < 1 million years after the beginning of the Solar System. This rapid formation of Jupiter acted as an effective barrier against inward transport of material across the disk, potentially explaining why our Solar System lacks any super-Earths ([Izidoro et al. 2015](#)). We can infer that for the Proxima Centauri system a Jupiter would dominate the system, because it would not have left enough mass in the disk to form PCb.

2.2 Study on the dynamics of exocomets

The initial conditions used for the comets in the Proxima Centauri system are based on the setup used in [Loibnegger et al. \(2017\)](#), who assumed that every system hosting planets also possesses reservoirs of cometary bodies. These reservoirs are produced during the phase of planet formation and are later disturbed by e.g., a passing star or the galactic tide which throws the comets towards the central star as studied by [Kaib et al. \(2013\)](#). This was done for the Solar System and the Oort cloud in the work of [Fouchard et al. \(2010\)](#). [Fouchard et al. \(2017\)](#) introduced a new kind of Oort cloud model; it originates from an Oort cloud precursor in form of a scattered disk with perihelia between Uranus and Neptune. The objects are launched into orbits with low inclinations and semi-major axes larger than 1000 au. However, close passing stars may induce comet showers. [Mamajek et al. \(2015\)](#) could show that 70000 years ago a low mass binary (HIP 85605) passed the Solar System at around 50000 au (which is at the boundary of the outer Oort cloud). [Loibnegger et al. \(2017\)](#) investigated the dynamics of comets in the system of HD 10180 and estimated probabilities for collisions and close encounters with the planets and discussed the possibility of a capture of comets in close-in orbits.

For our investigations we used the following dynamical configurations which are presented in Fig. 2:

- C1:** Star–planet b–planetesimal cloud
- C2:** Star–planet b–planet c–planetesimal cloud
- C3:** Star–planet b–planetesimal cloud–binary
- C4:** Star–planet b–planet c–planetesimal cloud–binary

As mentioned in the introduction, a second planet in the system is possible. From the work of [Kopparapu et al. \(2014\)](#) we know that PCb lies at the inner border of the HZ. The location of planet c is subject to the stability analysis performed in section 3.1. Because of a possible dry PCb we set the second planet at 0.119 au which is close to the outer border of the habitable zone.

The planetesimal cloud consists of 5000 objects which are uniformly distributed in the orbital inclinations. We start the comets on highly elliptic (almost parabolic) orbits. Therefore we set the initial conditions such that the perihelion distance $q < a_2 = 0.0485$ au and defined the following regions in cometary semi-major axes:

- R1:** 10-20 au
- R2:** 40-50 au
- R3:** 90-100 au
- R4:** 190-200 au
- R5:** 490-500 au
- R6:** 990-1000 au

Region **R1** is closest to PCb and represents the short period comets and is the analogue to the Kuiper Belt of our solar system. These short-period comets may have delivered water and other volatiles to Earth and the other terrestrial planets. However, such exocomets were found in a binary system by [Xu et al. \(2017\)](#). The outer regions were chosen to investigate the interaction with α Centauri and because the lack of knowledge about the size of the protoplanetary disk. Recent observations of Proxima Centauri showed a belt of dust orbiting around distances ranging between 1 and 4 au, approximately ([Anglada et al. 2017](#)). There are additional

signs for an outer extremely cold (about 10 K) belt around the star at about 30 au which is in the range of our simulations.

Hill sphere

Hill’s criterion offers a convenient approximation for the stability of planetary systems, like in the work of [Hamilton & Burns \(1992\)](#). The Hill sphere of Proxima Centauri (PC) is defined as the space where its gravitational attraction exceeds that of α Centauri (α C). We use the Hill radius of Proxima Centauri as a valid criterion for the ejection of comets from the star–binary system. The Hill radius for Proxima Centauri is defined as²:

$$R_{\text{Hill}} = a_{\text{bin}}(1 - e_{\text{bin}}) \sqrt[3]{\frac{M_{\text{PC}}}{3M_{\alpha\text{C}}}} \approx 1178.3 \text{ au.} \quad (2)$$

We assumed the semi-major axis of the outermost region (**R6**) smaller than the Hill radius ($R_{\text{Hill}} \approx 1200$ au).

We studied the restricted N-body problem for an integration time from $T_c = 3.3 \times 10^6$ (for the inner region **R1-R3**) up to $T_c = 6.6 \times 10^7$ periods of PCb (for the outer regions **R4-R6**). The equations of motion for all configurations were solved with the Radau method ([Everhart 1974, 1985](#)) from the Mercury integrator package ([Chambers 1999](#)). Unlike the famous hybrid-symplectic integrator of [Chambers \(1999\)](#), the Radau integration method is also well suited for studying binary star systems. The 15th order Radau method uses Gauss-Radau quadratures to integrate a time series by fitting an empirical curve to force evaluations at several unevenly-spaced points ([Everhart 1974](#)). Thus, this method is well suited for studying close approaches where a variable step-size adjustment is mandatory.

In our simulations we measured the number of:

- (i) Ejected comets
- (ii) Impacts onto the star
- (iii) Direct impacts on the planets b and c
- (iv) Close encounters with the planets b and c
- (v) Comets involved in close encounters
- (vi) Minimum orbital intersection distance (MOID) with the planets b and c
- (vii) Unique MOID impact events (only the involved comets)

A close encounter with the planet is defined when a comet enters 3 times the Hill radius of PCb. Comets with semi-major axes $a > R_{\text{Hill}} \approx 1200$ au are considered to be ejected.

2.3 Water transport

We simulated orbits of icy objects initially located in a cloud for different distances to PCb. Possible water transport can be inferred by impacts and by close encounters with the planet. In case of close encounters the comets can fractionate and collide with the planet as meteor showers like on Earth.

² The equation depends on the separation a_{bin} from Proxima to α Centauri, the eccentricity e_{bin} of Proxima Centauri around α Centauri, the mass of Proxima Centauri M_{PC} and the binary $M_{\alpha\text{C}}$ given in solar masses.

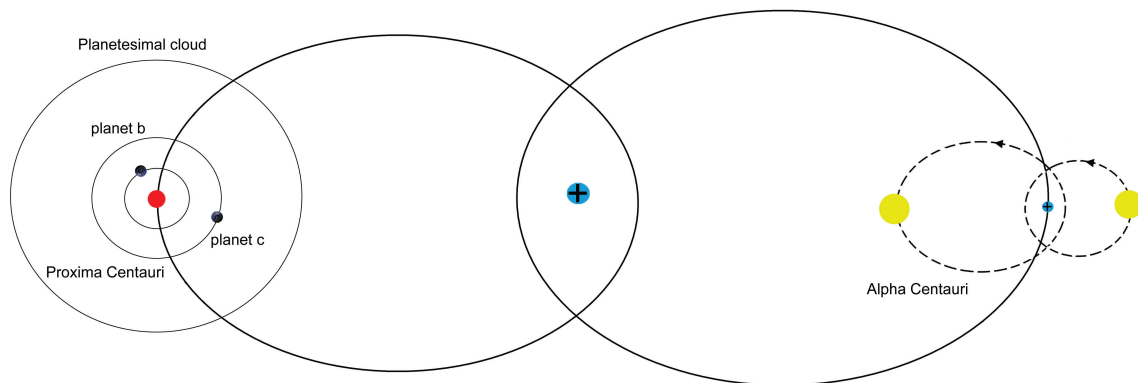


Figure 2. Illustration of the four configurations (C1-C4) used for our simulations. The mean distance from Alpha Centauri to Proxima Centauri is $a_{\text{bin}} = 8700$ au and the eccentricity $e_{\text{bin}} = 0.5$. The distance of planet b (PCb) is $a_2 = 0.0485$ au, while that of planet c (candidate) is $a_3 = 0.119$ au at the outer border of the HZ. The six different distances of the planetesimal cloud (only marked as one circle outside the planets' orbits) are listed in this section.

The details of how meteor showers are linked to comets and may have seeded the Earth with ingredients that made life possible is discussed in the work of Jenniskens (2006).

We define two impact indicators: direct impacts and minimum orbit intersection distance (MOID). Direct impacts are retrieved from the simulations for specific impact configurations, that means according to the real location of the two colliding bodies on their trajectory. This indicator gives a lower estimate of the impact rate. The second indicator, the MOID algorithm (Sitarski 1968), is widely used in celestial mechanics to determine whether an object can be a potential danger for the Earth or not. The MOID corresponds to the closest distance between keplerian orbits of two objects, regardless of their real position on their respective trajectories, considering all possible true anomalies leading to collisions. It is therefore appropriate to use the MOID for systems like Proxima Centauri where we don't know exactly the parameter space (planets and comets). For this purpose, we calculated the MOID after the numerical simulations as in Bancelin et al. (2017) for each comet and estimated the impact probability: each close encounter between the comet and the planet was analyzed by sampling their true anomalies in order to derive impact distances. Trajectories with $\text{MOID} < R_{\text{Prox}}$ were classified as impacts, where R_{Prox} corresponds to 1.08 Earth radii and is the estimated radius of PCb for an Earth-like composition (Brugger et al. 2016).

3 RESULTS

3.1 Investigation of an additional planet

In this section we present the results of our dynamical investigations concerning a possible second planet in the Proxima Centauri system. We studied the stability of an additional planet placed from $a_3 = 0.06$ au (orbital period 15 days) up to an initial semi-major axis of $a_3 = 0.3$ au (orbital period 173 days), for eccentricities up to $e_3 = 0.5$. The second signal mentioned by Anglada-Escudé et al. (2016) falls into the orbital period range 60–500 days, i.e. in the semi-major axis interval 0.15–0.7 au. Fig. 3 shows the stability maps for the

Table 2. Number of stable orbits and the percentage for all calculated stability maps.

e_2	mass (M_{PCb})	number of stable orbits	percent of stable orbits
0.0	1	380	86.2
0.1	1	384	87.1
0.2	1	390	88.4
0.3	1	383	86.8
0.0	5	345	78.2
0.1	5	369	83.7
0.2	5	373	84.6
0.3	5	342	77.6

case of $5M_{\text{Prox}}$. Each stability map represents different values of eccentricity (e_2) starting from $e_2 = 0$ to $e_2 = 0.3$. In Fig. 3 (lower right graph) we marked the 2:1 and 3:1 mean motion resonances (MMRs) with PCb. We conclude that the stable region is quite large. In addition we counted the number of stable orbits for each stability map (grid size = 21×21) which is summarized in table 2. We show that the percentage of stable orbits for one M_{Prox} is very similar for the different eccentricities (e_2) and has a mean value of 87 ± 1 %. This is also true for $5M_{\text{Prox}}$ where the mean value is 81 ± 4 %. In addition, we tested the stability for $10M_{\text{Prox}}$ and did not find any significant difference to the $5M_{\text{Prox}}$ case.

Finally we can conclude that:

- (i) The largest unstable region was found for the largest eccentricity of PCb ($e_2=0.3$).
- (ii) The stability maps with an initial eccentricity of $0 < e_2 < 0.2$ are similar.
- (iii) The stability maps are varying only slightly with the mass of the planets b and c.
- (iv) For $0 < e_3 < 0.2$ almost all orbits are stable.
- (v) The 2:1 and 3:1 MMR are visible for an initial eccentricity of PCb $e_2=0.3$.

The stability maps in Fig. 3 indicate that Proxima Centauri could indeed host two planets in a compact configuration. To reinforce this impression we made use of the Hill

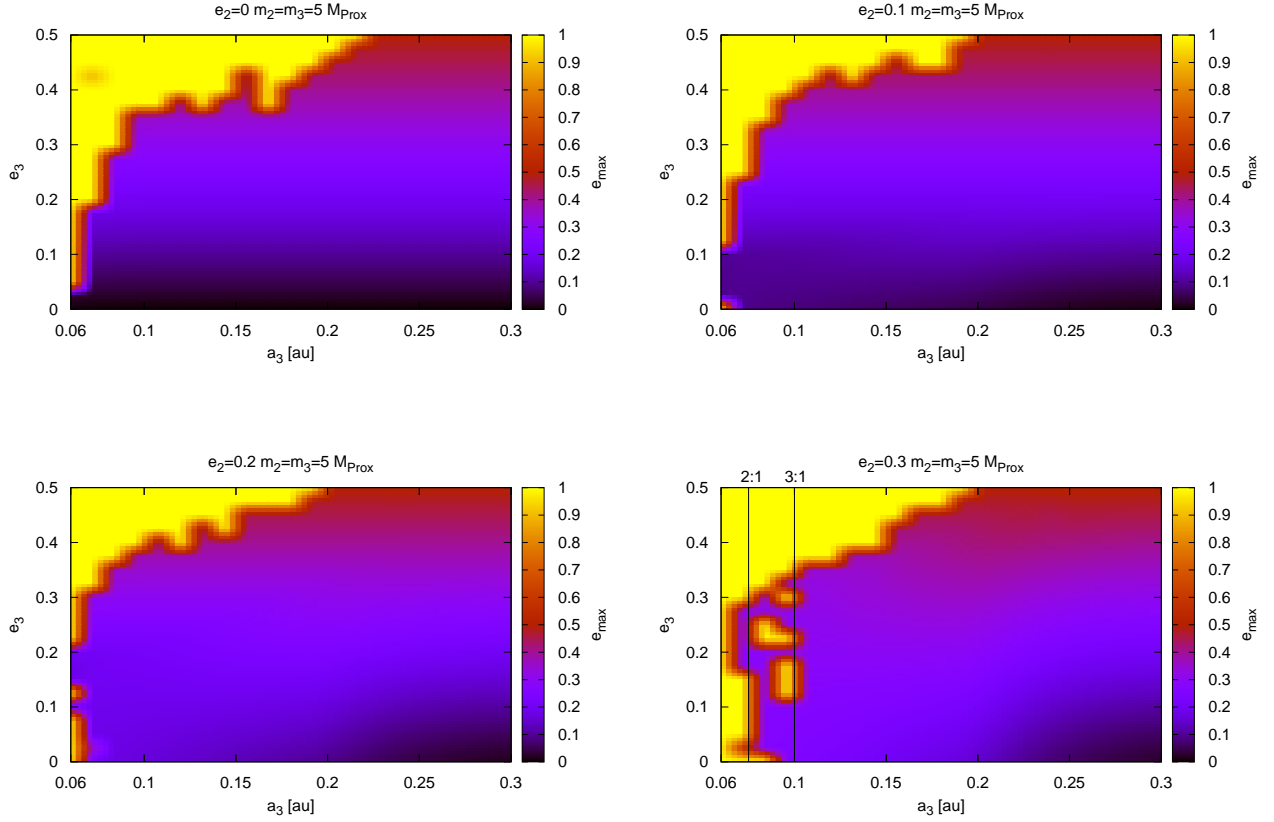


Figure 3. Stability maps of PCb presenting the size of the stable region which depends on the initial semi-major axis a_3 and the eccentricity of planet c (e_3). The masses of the planets are equal $m_2=m_3=5M_{\text{Prox}}$. The 2:1 and 3:1 mean motion resonances are marked in the lower right graph for $e_2=0.3$. The colour code presents the values of e_{max} . The yellow and red regions depict large values of e_{max} (corresponding to unstable or chaotic motion), whereas the violet and black regions represent small ones.

stability criterion of Gladman (1993). This criterion establishes estimates for the Hill stability of two close planets in a full three-body problem. If both planets would move on circular orbits then planet c must move at $a_c > 0.053$ au in order to satisfy the Hill stability criterion. This condition is comfortably fulfilled by our choice of setting PCc initially to $a_c = 0.119$ au, which is more than two times the required separation from PCb. Increasing the masses of both planets symmetrically the critical separation also increases; for $m_1 = m_2 = 5M_{\text{Prox}}$ and still circular motion the minimum value of the critical separation is $a_c = 0.056$ au, while for eccentric orbits this value increases to $a_c = 0.062$ au. See Fig. 4 for the representation of a_c as a function of M_{Prox} , as well as its dependence on the initial eccentricity. In a recent work Petrovich (2015) developed a new stability criterion by the help of long term integrations (10^8 peroids) for the three-body-problem discussing exoplanetary systems. By applying this criterion we found out that PCc could have eccentricities up to $e_3=0.3$ which confirms our results presented in Fig. 3. In summary, according to this criterion it is safe to choose a separation between the two planets such as that described above.

3.2 Study on the dynamics of exocomets

3.2.1 Investigation of one and two planets

In this study we investigated the influence of the binary (α Centauri) on the water transport onto PCb and a possible second planet orbiting in the HZ.

In table 3 (upper part) we present the results for **C1** (Star – planet b – planetesimal cloud) for the inner three regions of the planetesimal cloud. The number of ejected comets and of the impacts on the star decreases the quantity of water transported to PCb, whereas impacts on the planet and close encounters with the planet increases the water transport. The number of ejected comets increases with larger distance to the host star; region **R3** has the largest number. However, the number of collisions with the star is almost equal. We have the largest number of close encounters for the inner planetesimal cloud (region **R1**) and decreases for the outer ones, but the number of involved comets does not differ much (around 80 %). In the next step we included a second planet in **C2** which is shown in table 3 (lower part). It is visible that the region **R1** has more impacts and close encounters than the other regions for both configurations. We can conclude that there is no difference in the total number of impacts with the planet

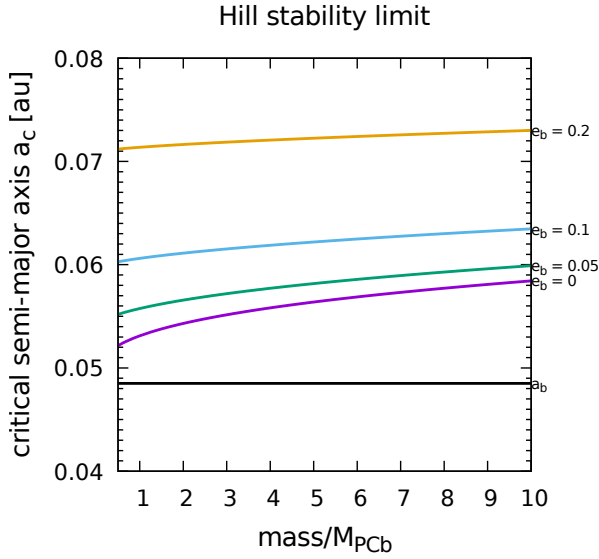


Figure 4. The estimates of the Hill stability limit of two close planets after Gladman (1993). The parameter e_2 is the initial eccentricity of the planet PCb. The x-axis is scaled in units of the mass of PCb.

between **C1** and **C2**. When we summarize the number of impacts onto planets b and c we have almost the same number as for **C1** (**C1**: 7,1,3 and **C2**: 7,3,0). However, planet b has consistently more impacts in **C2** than planet c, which is valid for all regions as shown in the tables 3, 4, 5 and is well visible in the impact probability summarized in table 6. It seems that the number of impacts will be split if the planets have the same mass without any outer perturber. The number of MOID impacts is much smaller than the number of close encounters³, but still many MOID impacts remain; this is valid for both configurations. We can conclude that the further away the planetesimal clouds from the planets the smaller will be the number of impacts, close encounters and MOID impacts.

In a next step we prepared a distribution of the number of close encounters by counting the number of involved comets. In Fig. 5 (left graph) we present the distribution of all close encounters for the configuration **C1** for the inner three regions. In the right graph of Fig. 5 we present these distributions excluding the ejected comets and the ones which have impacts with the host star. When we compare these two graphs we can conclude that the distribution is almost the same for the inner region (**R1**). Whereas for larger distances (e.g. the outer regions **R2**, **R3**) we found that the difference of number of close encounters increases.

One can see that many of the involved comets only have relatively few close encounters. A large number of close encounters implies that the comet would be disrupted and/or de-volatilized and would not contribute to water transport to the planet.

In addition the distribution shows that for region **R1** the number of involved comets is almost constant. For the regions **R2** and **R3** the number of close encounters rises at

Table 3. Summary of the results for **C1** (planet b) and **C2** (planets b and c). For each region and configuration we calculated 5000 objects.

number	R1	R2	R3
C1			
Ejected comets	463	890	1461
Collisions with the star	251	288	288
Impacts on the planet b	7	1	3
Close encounters	920187	220924	103269
Comets involved	4110	4158	4068
MOID impacts	9352	2733	1748
Unique MOID impacts	173	86	76
C2			
Ejected comets	589	1001	1566
Collisions with the star	389	542	573
planet b			
Impacts on the planet	5	3	0
Close encounters	979909	214073	199280
Comets involved	4205	4156	3940
MOID impacts	8608	2294	2386
Unique MOID impacts	286	117	89
planet c			
Impacts on the planet	2	0	0
Close encounters	821745	168836	181796
Comets involved	4172	3883	3521
MOID impacts	1398	484	643
Unique MOID impacts	195	63	33

a small number edge, which means that most comets have only a few close encounters with the planet.

For the estimate of the water transport by comets we have to investigate the impact velocity, which we present as histograms in Fig. 6. In the left graph we presented the impact velocities for all encounters. For region **R3** one can see that the histogram has two maxima: the left one represents the impacts of comets with prograde motion whereas the right peak represents the retrograde comets with larger velocities.

3.2.2 Calculations including α Centauri

We analysed the cometary dynamics by means of residence time maps (after Bottke et al. 2002) in the osculating aphelion distance Q –perihelion distance q space (as shown in Fig. 7). Each cell gives the normalized frequency of the comets of the map where brighter colours indicate higher residence time. Any comet with constant aphelion distance but varying perihelion distance due to close encounters with the planets is represented by a vertical stripe. The dashed lines show the perihelion limits for encounters to the planets PCb and PCc. Note that in configuration **C4** many comets are scattered to larger perihelion distance; beyond the border of PCc. That indicates that the binary influences the dynamics of the Proxima Centauri system. To show the effects of the binary system α Centauri we compared the different configurations (**C1**–**C4**) which are summarised in table 3 and table 4. First, we can see that the number of ejected comets is smaller for **C3** compared to **C1**, whereas the number of collisions with the star increased for **C3**. This is also valid when we compare configuration **C4** with **C2**. We have to mention that the ejection distance for **C3** and **C4** is 20000 au

³ ~1% of close encounters lead to an MOID impact

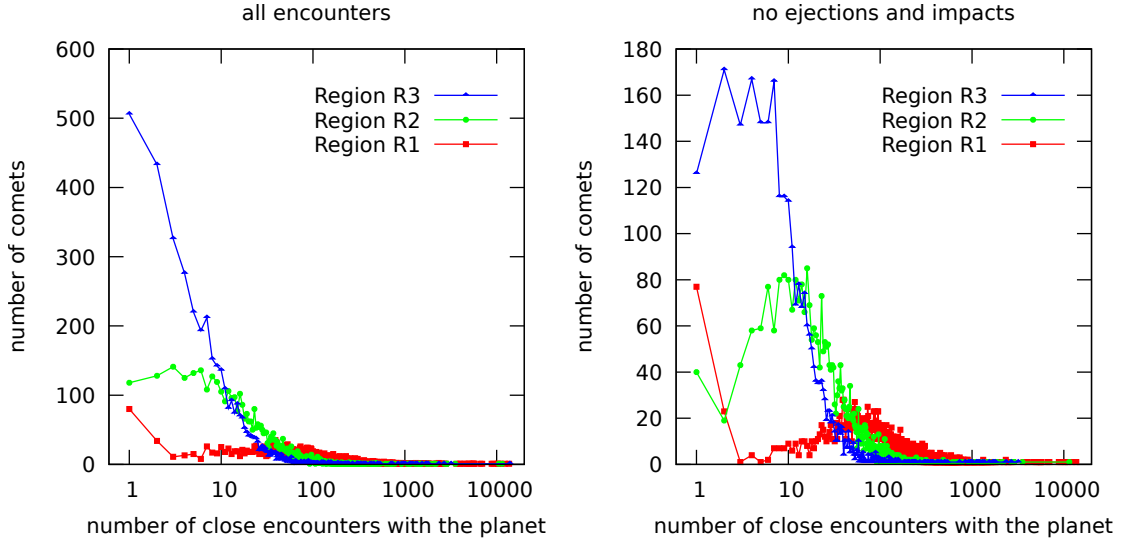


Figure 5. Distribution of the number of close encounters with planet b depending on the number of involved comets for the configuration **C1** with different planetesimal clouds for the inner 3 regions (red line for region **R1**: 10-20 au, green for **R2**: 40-50 au and blue for **R3**: 90-100 au). Therefore we counted the number of close encounters for all 5000 objects. It shows that the outer region has more comets with a smaller number of close encounters than the inner ones. The left graph represents all close encounters whereas the right graph shows the same, but without the ejected comets and the ones which have impacts with the host star.

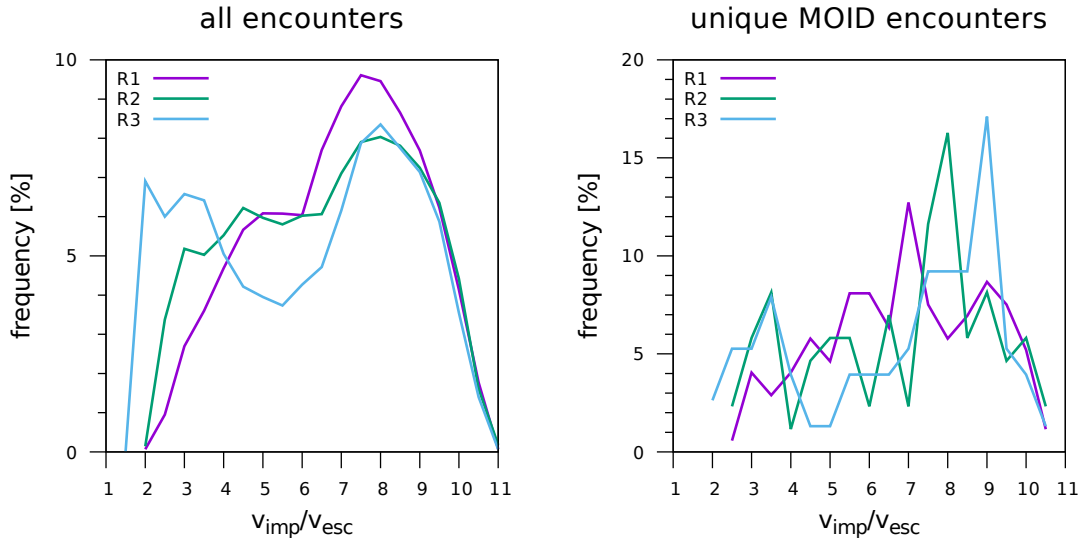


Figure 6. Histogram of the impact velocity for different regions of the planetesimal cloud. Left graph: all close encounters; right graph only taking into account the very first MOID encounter.

instead of approximately 1200 au (Hill radius) before. Due to the restricted simulation time this causes that some hyperbolic comets are far away but not yet considered to be ejected. The number of impacts with one planet (**C1** and **C3**) is similar, as in comparison of **C2** with **C4** with two planets. But the number of close encounters for the configurations (**C3**, **C4**) including α Centauri is slightly higher than without the binary system (**C1**, **C2**), as well as the number of involved comets. However, the number of MOID impacts increases significantly when we compare **C3** with **C1** and **C4** with **C2**. Therefore we can conclude that the influence of α Centauri in (**C3**, **C4**) on the possible water

transport is measurable, and mainly visible in the number of unique MOID impact events.

3.2.3 Investigation of the outer regions

Table 5 shows the dynamical study with a possible planetesimal cloud further out represented by the regions **R4**, **R5** and **R6**. These studies were done for configuration 4 which includes α Centauri and a second planet. For the outer regions we increased the integration time to $T_c=6.6 \cdot 10^7$ periods of PCb, to make sure to cover several periastron passages of α Centauri. One can see that the planetesimal cloud for region

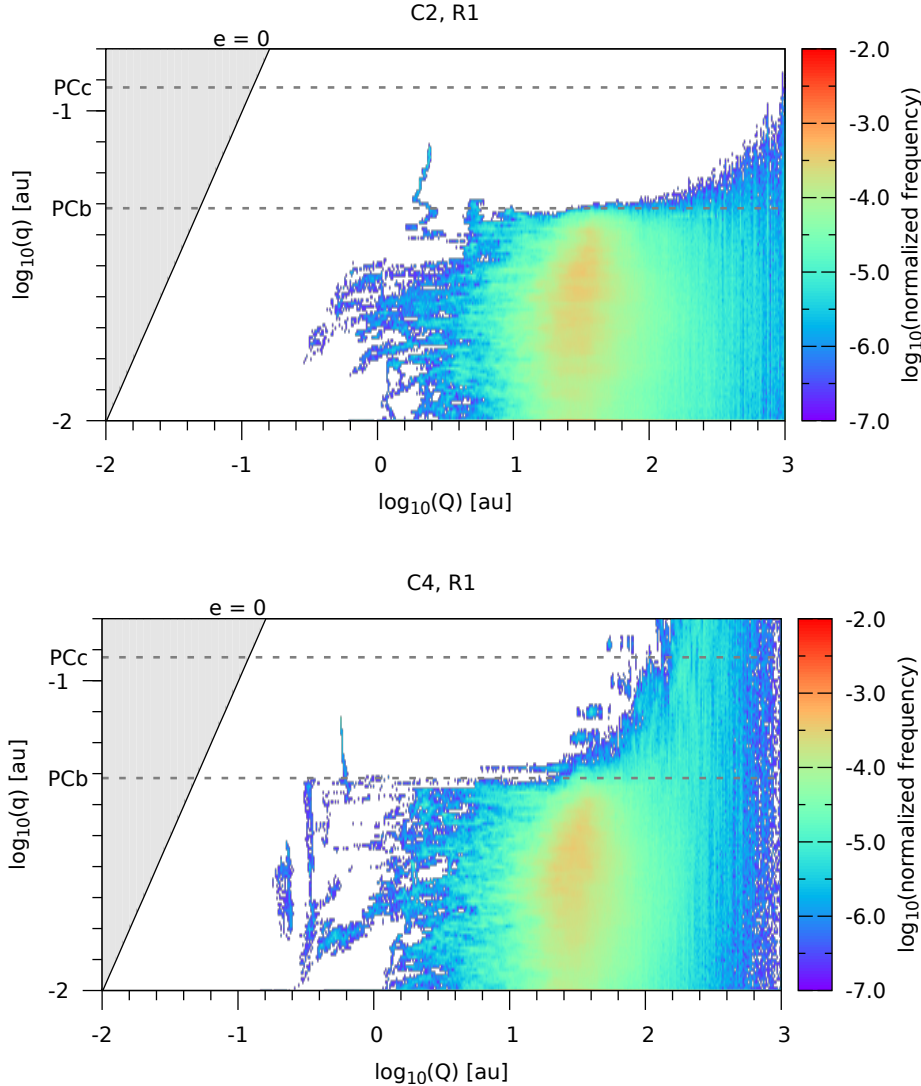


Figure 7. Distribution of the residence times of all involved comets for the configuration **C2** (upper graph) and **C4** (lower graph) for the region **R1**. We plot the logarithm with the aphelion distance Q versus the perihelion distance q . The colour code of the figure is the normalized frequency of the comets to reside in a certain cell of the grid.

R6 (1000 au) is heavily depleted by ejections and collisions with the star. Therefore and because of the close encounters, MOID, and impacts we can conclude that from region **R6** no water transport is possible. The comets of all regions have only impacts with Proxima Centauri. Region **R5** shows similar results except some close encounters with the planets are possible.

However, region **R4** has less ejected comets and collisions with the star. We expect some limited water transport because of the number of impacts (three in total), close encounters with the planets and the MOID. Because of region **R4** we expect that the limit for water transport is around 200 au. Further intense investigations are necessary to obtain a better estimate of this outer limit.

3.3 Water transport

To estimate the amount of water transported by comets to the planets b and c we concentrate on impacts as the most efficient transport mechanism. We can estimate how much water may be transported for the different configurations by the following equation:

$$W_{\text{H}_2\text{O}} = M_{\text{tot}} \times wmf \times P(q \leq a_p) \times P(I) / M_{\text{H}_2\text{O}}. \quad (3)$$

In this expression the different factors are either derived from the simulations – such as the impact probability $P(I)$ – or they are model dependent like the water mass fraction (wmf).

The first element is the total mass M_{tot} of each region R_i ($i = 1 \dots 6$). This total mass is calculated by integrating the surface density profile (Crida 2009; Ciesla et al. 2015) $\Sigma(r) = \Sigma_0 (r/1\text{AU})^{-\alpha}$ with the parameters (α, Σ_0) . We assume an exponent $\alpha = 3/2$ which results in a radial decrease of the

Table 4. Summary of the results for **C3** and **C4** where the planetary system is perturbed by the binary system α Centauri. For each region and configuration we calculated 5000 objects. *There are no collisions with α Centauri, only with Proxima Centauri.

number	R1	R2	R3
C3			
Ejected comets	94	104	90
Collisions with the star*	377	555	567
Impacts on the planet b	7	5	2
Close encounters	895277	261929	155429
Comets involved	4173	4533	4043
MOID impacts	7033	4073	2762
Unique MOID impacts	264	257	131
C4			
Ejected comets	103	134	105
Collisions with the star*	467	674	741
planet b			
Impacts on the planet	8	1	0
Close encounters	1270364	200499	132931
Comets involved	4207	4445	3809
MOID impacts	9086	1771	1446
Unique MOID impacts	405	284	117
planet c			
Impacts on the planet	1	0	0
Close encounters	1091422	166790	118335
Comets involved	4085	4174	3749
MOID impacts	2222	304	320
Unique MOID impacts	230	85	43

Table 5. Results for scenario **C4** where the planetary system is perturbed by the binary system α Centauri, but for the outer regions **R4**, **R5** and **R6**. For each region we calculated 5000 objects. *There are no collisions with α Centauri only with Proxima Centauri.

Regions	R4	R5	R6
Ejected comets	493	127	1368
Collisions with the star*	834	979	1733
planet b			
Impacts on the planet	2	0	0
Close encounters	8043	23	0
Comets involved	155	6	0
MOID impacts	169	0	0
Unique MOID impacts	25	0	0
planet c			
Impacts on the planet	1	0	0
Close encounters	9494	19	4
Comets involved	256	13	1
MOID impacts	56	0	0
Unique MOID impacts	20	0	0

total mass, while the value $\Sigma_0 = 30 \text{ g cm}^{-2}$ describes the surface density for a mixture of solids plus ice, and is valid for regions beyond the system’s snow line (Hayashi 1981).

The water mass fraction wmf was chosen to be around 50 percent following Ciesla et al. (2015). This value is rather high compared to the typical wmf of asteroids (5–10 %). Since all our source regions are situated beyond the snow line we can expect this large water content to be reasonable.

In order to determine the amount of the total stored water in each region that is able to be transferred to the planets

we need to assess the transport probability $P(q \leq a_p)$, i.e. the fraction of comets achieving highly elliptic orbits that take them to pericenter distances q interior to the planet’s orbit a_p . From the eccentricity distributions⁴ for trans-Neptunian objects (TNOs) and long-period comets (LPCs) we can infer that this fraction is between 0.01 (TNOs) and 0.3 (LPCs). However, the latter value is probably biased since only objects from the high-eccentricity tail of the distribution will reach the inner parts of the Solar System and become visible. Therefore we select $P(q \leq a_p) = 0.01$ as a more realistic estimate.

The impact probability $P(I)$ is described by two sets of values. We estimate the lower limit of the water mass transport to the planets by using the probabilities for direct impacts. As an upper limit we use the probabilities for the unique MOID impacts. The actual water mass will be expected to lie in the range between these two extremal values.

Note that in Eq. (3) the transported water mass $W_{\text{H}_2\text{O}}$ is scaled in units of one Earth ocean mass, $M_{\text{H}_2\text{O}} = 1,5 \times 10^{21} \text{ kg}$.

In Fig. 7 we show that comets can reach very close to the host star ($q \leq 0.01 \text{ au}$). This leads to the question of water (ice) loss by sublimation due to the stellar radiation. We can estimate the sublimation mass flux (Jewitt 2012; Bancelin et al. 2017) averaged over one orbit as well as over the lifetime of a comet (in the simulations). In both cases the result is that this loss mechanism is irrelevant over the simulation time-span. Sublimation should be maximal during pericenter passage, but at a typical eccentricity $e > 0.99$ the whole passage through the Proxima Centauri habitable zone takes less than about 10 days. We have to compare this period of time with the orbital periods, which are typically of the order of hundreds of years. Hence these highly eccentric comets spend much time at large distances to the star where the temperature is too low for any significant sublimation. Therefore we did not consider this water loss process.

The results are presented in table 6, where the conservative minimum water mass transport represented by direct impacts can be up to 0.6 Earth oceans. Whereas, the optimistic water transport represented by MOID impacts can rise up to 30 Earth oceans.

4 CONCLUSIONS

In this paper, we first investigated the dynamical possibility of a second planet in Proxima Centauri. We excluded an outer gas giant in our studies because we do not expect another planet with Saturn or Jupiter mass as shown in the radial velocity limits of Fig. 1. Therefore, we did several numerical simulations and found that both planets could be stable even for large planetary masses (1, 5 M_{Prox} , and 10 M_{Prox}) and large eccentricities of the second planet (up to $e_3 = 0.3$). We found the 2:1 and 3:1 MMR for larger eccentricities $e_2 = 0.3$ of Proxima Centauri b (PCb) as shown in Fig. 3 lower right graph. From Fig. 3 we can conclude that the second planet can be very close to PCb like in a compact planetary system (Funk et al. 2010).

⁴ Based on data from the JPL Small-Body Database Search Engine, https://ssd.jpl.nasa.gov/sbdb_query.cgi

Table 6. Summary of the impact probability of direct impacts with the planets. PCb represents planet b and PCc a possible second planet c. The second part represents the amount of water transported to the planets given in units of Earth ocean masses.

Impact probability	C1		C2		C3		C4	
	PCb	PCb	PCc	PCb	PCb	PCc	PCb	PCc
	$\cdot 10^{-4}$							
Direct impacts								
R1	14	10	4	14	16	2		
R2	2	6	< 2	10	2	< 2		
R3	6	< 2	< 2	4	< 2	< 2		
Unique MOID impacts								
R1	346	572	390	528	810	460		
R2	172	234	126	514	568	170		
R3	152	178	66	262	234	86		
Water transport in Earth oceans by direct impacts								
R1	0.52	0.37	0.15	0.52	0.59	0.07		
R2	0.04	0.13	0.00	0.21	0.04	0.00		
R3	0.09	0.00	0.00	0.06	0.00	0.00		
Water transport in Earth oceans by unique MOID impacts								
R1	12.81	21.18	14.44	19.56	30.00	17.04		
R2	3.63	4.94	2.66	10.85	11.99	3.59		
R3	2.21	2.58	0.96	3.80	3.40	1.25		

The observation of proto-planetary disks around small stars is difficult, for this reason we don't know the mass and the extension of such disks and the evolution of possible outer comet clouds. Therefore we made several simulations where we changed the distance of the planetesimal cloud to the host star. In the next step, we investigated the influence of the binary (α Centauri) on the water transport onto PCb and a possible second planet orbiting in the HZ. In case that the planet PCb is too dry, maybe a second planet at the outer border of the habitable zone will have a higher probability to be habitable. We found that the water transport onto planets b and c by direct impacts is rare (except region **R1**), compared with MOID impacts. Our simulations showed in addition that planet b would gain more water than planet c, by the help of direct (impacts) or indirect (close encounters) water transport. The impact probabilities estimated from the direct impacts are summarized in table 6 and show that the inner region has a larger water transport (especially region **R1**) than the outer ones. We can conclude that α Centauri perturbs the system, but does not increase the influx of comets and therefore the water transport is not significantly larger. By studying the outer regions we found out that the limit for water transport is around 200 au for Proxima Centauri. The planetesimal cloud disappeared for region **R5** almost entirely and for region **R6** completely. The observations of dust belts around Proxima Centauri strengthen the idea of water transport by icy objects from debris disks as shown in [Anglada et al. \(2017\)](#). We presume that these results could be important for Proxima like systems.

Further investigations have to be done to solve questions like: If α Centauri were close to Proxima Centauri how much would that influence the system. Could there be an exchange of comets between α Centauri and Proxima Centauri and to which extent would that be?

This work will possibly help to understand the cosmogony of Proxima Centauri and the dynamics of water transport in M-star systems in general; however, further investigations will be necessary.

ACKNOWLEDGEMENTS

The authors thank Prof. Giovanni Valsecchi and Prof. Christos Efthymiopoulos for their valuable comments. R. Schwarz wants to acknowledge the support by the Austrian FWF projects P23810-N16, S11608-N16 and S11603-N16. E. Pilat-Lohinger, D. Bancelin, and Á. Bazsó want to acknowledge the support from the Austrian FWF project S11608-N16. R. Dvorak, B. Loibnegger, and T. Maindl want to acknowledge the support from the Austrian FWF project S11603-N16. K. Kislyakova wants to acknowledge the support from the FWF project S11607-N16. We thank the High Performance Computing Resources team at New York University Abu Dhabi and especially Jorge Naranjo for helping us carry out our simulations.

REFERENCES

- Altwegg K., et al., 2015, *Science*, **347**, 1261952
 Anglada-Escudé G., et al., 2016, *Nature*, **536**, 437
 Anglada G., et al., 2017, preprint, ([arXiv:1711.00578](#))
 Bancelin D., Pilat-Lohinger E., Maindl T. I., Ragossnig F., Schäfer C., 2017, *AJ*, **153**, 269
 Barnes R., Jackson B., Greenberg R., Raymond S. N., 2009, *ApJ*, **700**, L30
 Beust H., Vidal-Madjar A., Ferlet R., Lagrange-Henri A. M., 1990, *A&A*, **236**, 202
 Bottke W. F., Morbidelli A., Jedicke R., Petit J.-M., Levison H. F., Michel P., Metcalfe T. S., 2002, *Icarus*, **156**, 399
 Brugger B., Mousis O., Deleuil M., Lunine J. I., 2016, *ApJ*, **831**, L16
 Chambers J. E., 1999, *MNRAS*, **304**, 793
 Ciesla F. J., Mulders G. D., Pascucci I., Apai D., 2015, *ApJ*, **804**, 9
 Coleman G. A. L., Nelson R. P., Paardekooper S. J., Dreizler S., Giesers B., Anglada-Escudé G., 2017, *MNRAS*, **467**, 996
 Crida A., 2009, *ApJ*, **698**, 606
 Eggl S., Dvorak R., 2010, in Souchay J., Dvorak R., eds, *Lecture Notes in Physics*, Berlin Springer Verlag Vol. 790, *Lecture Notes in Physics*, Berlin Springer Verlag. pp 431–480, [doi:10.1007/978-3-642-04458-8_9](#)
 Eiroa C., et al., 2016, *A&A*, **594**, L1
 Everhart E., 1974, *Celestial Mechanics*, **10**, 35
 Everhart E., 1985, in Carusi A., Valsecchi G. B., eds, *Dynamics of Comets: Their Origin and Evolution*, Proceedings of IAU Colloq. 83, held in Rome, Italy, June 11–15, 1984. Edited by Andrea Carusi and Giovanni B. Valsecchi. Dordrecht: Reidel, Astrophysics and Space Science Library. Volume 115, 1985, p.185. p. 185
 Fouchard M., Froeschlé C., Rickman H., Valsecchi G. B., 2010, in Souchay J., Dvorak R., eds, *Lecture Notes in Physics*, Berlin Springer Verlag Vol. 790, *Lecture Notes in Physics*, Berlin Springer Verlag. pp 401–430, [doi:10.1007/978-3-642-04458-8_8](#)
 Fouchard M., Rickman H., Froeschlé C., Valsecchi G. B., 2017, *Icarus*, **292**, 218
 Funk B., Wuchterl G., Schwarz R., Pilat-Lohinger E., Eggl S., 2010, *A&A*, **516**, A82
 Gladman B., 1993, *Icarus*, **106**, 247

Grady C. A., Sitko M. L., Bjorkman K. S., Pérez M. R., Lynch D. K., Russell R. W., Hanner M. S., 1997, *ApJ*, **483**, 449

Hamilton D. P., Burns J. A., 1992, *Icarus*, **96**, 43

Hanslmeier A., Dvorak R., 1984, *A&A*, **132**, 203

Hartogh P., et al., 2011, *Nature*, **478**, 218

Hayashi C., 1981, *Progress of Theoretical Physics Supplement*, **70**, 35

Izidoro A., Raymond S. N., Morbidelli A., Hersant F., Pierens A., 2015, *ApJ*, **800**, L22

Jenniskens P., 2006, *Meteor Showers and their Parent Comets*, ISBN 0521853494, Cambridge, UK: Cambridge University Press.. Cambridge University Press

Jewitt D., 2012, *AJ*, **143**, 66

Kaib N. A., Raymond S. N., Duncan M., 2013, *Nature*, **493**, 381

Kane S. R., Gelino D. M., Turnbull M. C., 2017, *AJ*, **153**, 52

Kervella P., Thévenin F., Lovis C., 2017, *A&A*, **598**, L7

Kiefer F., Lecavelier des Etangs A., Vidal-Madjar A., 2014a, in Ballet J., Martins F., Bournaud F., Monier R., Reylé C., eds, SF2A-2014: Proceedings of the Annual meeting of the French Society of Astronomy and Astrophysics. pp 39–43

Kiefer F., Lecavelier des Etangs A., Boissier J., Vidal-Madjar A., Beust H., Lagrange A.-M., Hébrard G., Ferlet R., 2014b, *Nature*, **514**, 462

Kislyakova K. G., et al., 2017, *Nature Astronomy*

Kopparapu R. K., Ramirez R. M., SchottelKotte J., Kasting J. F., Domagal-Goldman S., Eymet V., 2014, *ApJ*, **787**, L29

Kruijjer T. S., Burkhardt C., Budde G., Kleine T., 2017a, in Lunar and Planetary Science Conference. p. 1073

Kruijjer T. S., Kleine T., Burkhardt C., Budde G., 2017b, in Lunar and Planetary Science Conference. p. 1386

Lichtenegger H., 1984, *Celestial Mechanics*, **34**, 357

Loibnegger B., Dvorak R., 2017, in T. I. Maindl H. Varvoglis R. D., ed., Proceedings of the First Greek-Austrian Workshop on Extrasolar Planetary Systems. CreateSpace Independent Publishing Platform, ISBN: 1544255632, pp 125–136

Loibnegger B., Dvorak R., Cuntz M., 2017, *AJ*, **153**, 203

Mamajek E., 2017, preprint, ([arXiv:1710.11364](https://arxiv.org/abs/1710.11364))

Mamajek E. E., Barenfeld S. A., Ivanov V. D., Kniazev A. Y., Väisänen P., Beletsky Y., Boffin H. M. J., 2015, *ApJ*, **800**, L17

Mesa D., et al., 2017, *MNRAS*, **466**, L118

Mulders G. D., Ciesla F. J., Min M., Pascucci I., 2015, *ApJ*, **807**, 9

Nilsson R., et al., 2010, *A&A*, **518**, A40

Pawellek N., Krivov A. V., Marshall J. P., Montesinos B., Ábrahám P., Moór A., Bryden G., Eiroa C., 2014, *ApJ*, **792**, 65

Petrovich C., 2015, *ApJ*, **808**, 120

Pilat-Lohinger E., Eggl S., 2011, Publications of the Astronomy Department of the Eotvos Lorand University, **20**, 119

Ribas Á., Bouy H., Merín B., 2015, *A&A*, **576**, A52

Ribas I., et al., 2016, *A&A*, **596**, A111

Sándor Z., Süli Á., Érdi B., Pilat-Lohinger E., Dvorak R., 2007, *MNRAS*, **375**, 1495

Schwarz R., Süli Á., Dvorak R., 2009, *MNRAS*, **398**, 2085

Schwarz R., Funk B., Zechner R., Bazsó Á., 2016, *MNRAS*, **460**, 3598

Sitarski G., 1968, *Acta Astron.*, **18**, 171

Süli Á., Dvorak R., Freistetter F., 2005, *MNRAS*, **363**, 241

Vicente S. M., Alves J., 2005, *A&A*, **441**, 195

Wahlberg Jansson K., Johansen A., 2014, in Muinonen K., Penttilä A., Granvik M., Virkki A., Fedorets G., Wilkman O., Kohout T., eds, Asteroids, Comets, Meteors 2014.

Welsh B., Montgomery S. L., 2013, in American Astronomical Society Meeting Abstracts #221. p. 109.03

Willacy K., et al., 2015, *Space Sci. Rev.*, **197**, 151

Xu S., Zuckerman B., Dufour P., Young E. D., Klein B., Jura M., 2017, *ApJ*, **836**, L7

de la Fuente Marcos C., de la Fuente Marcos R., 2017, preprint, ([arXiv:1711.00445](https://arxiv.org/abs/1711.00445))

APPENDIX A: STABILITY

To confirm our results in section 3.1 (star-planet-planet) we used the stability catalogue “ExoCat” (after Sándor et al. 2007). The application “ExoCat” allows to check whether a newly discovered planet in a single-star single-planet system moves inside a stable region, using results of the work of Sándor et al. (2007) and Pilat-Lohinger & Eggl (2011). The simulations from “ExoCat” used the relative Lyapunov indicator (RLI) to investigate the stability of the system. The eccentricity of the planet PCb was set to $e_2=0$ for all stability maps. In that way we looked for the stability of an outer planet (PCc) as shown in Fig. 3. We compared the stability plots for two different mass ratios $\mu = 1 \times 10^{-4}$ and 2×10^{-4} ($\mu = m_2/(m_1 + m_2)$) and our calculations 1.7×10^{-4} .

This paper has been typeset from a $\text{\TeX}/\text{\LaTeX}$ file prepared by the author.

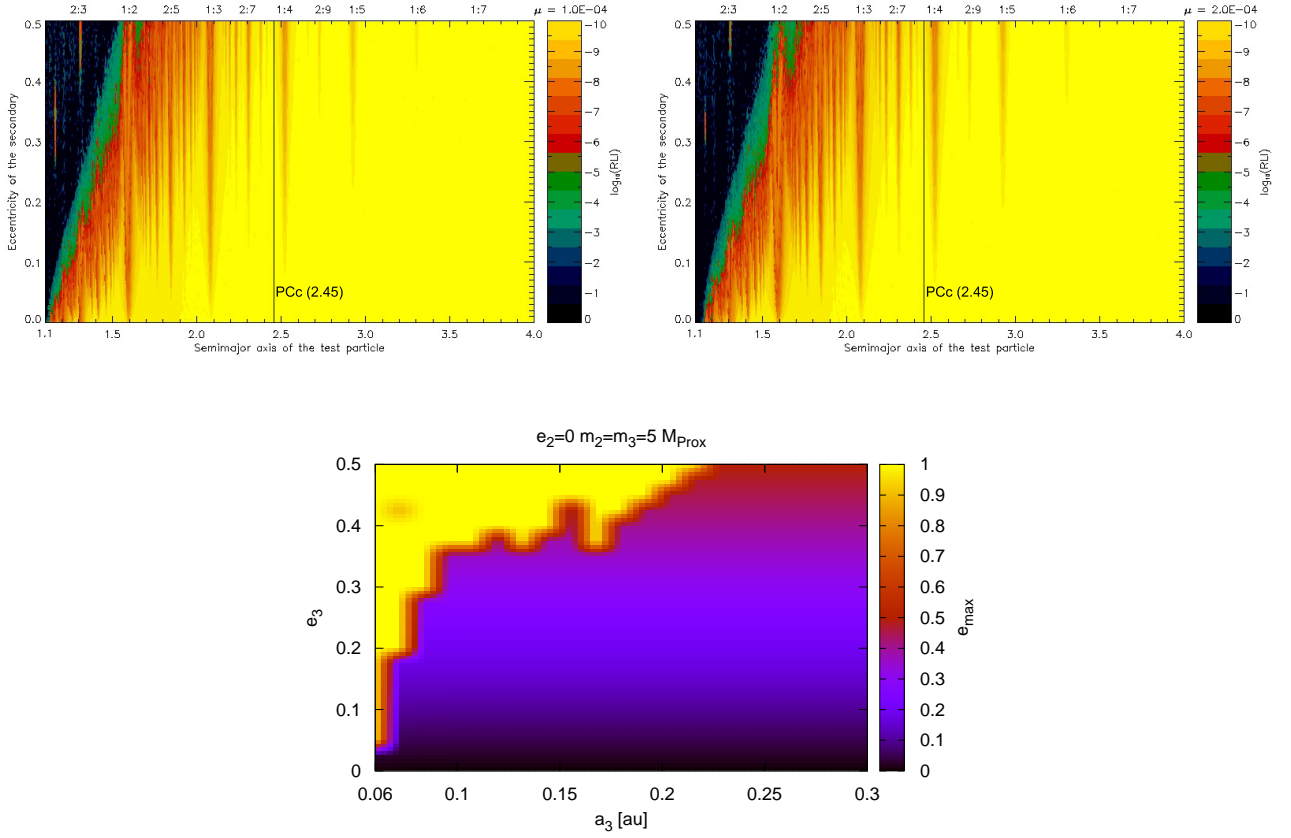


Figure A1. The upper graphs show the stability maps and the size of the stable region of “ExoCat” with a possible additional planet PCc for two different mass ratios ($\mu = 10^{-4}$ and $\mu = 2 \cdot 10^{-4}$). The masses of the planets are equal $m_2 = m_3 = 5 \cdot M_{\text{Prox}}$. The lower graph presents the stability maps of PCc with an additional inner planet PCb. The colour code presents the values of e_{\max} (lower graph) and the chaos indicator RLI (upper graphs) as given in the figures.